Schizophrenia Bulletin vol. 45 no. 2 pp. 415–424, 2019
doi:10.1093/schbul/sby039
Advance Access publication 5 April 2018

Data-Driven Analysis of Functional Connectivity Reveals a Potential Auditory Verbal Hallucination Network

Dustin Scheinost*[,1], Fuyuze Tokoglu[1], Michelle Hampson[1], Ralph Hoffman[2], and R. Todd Constable[1,3]

[1]Department of Radiology and Biomedical Imaging, Yale School of Medicine, New Haven, CT; [2]Department of Psychiatry, Yale School of Medicine, New Haven, CT; [3]Department of Neurosurgery, Yale School of Medicine, New Haven, CT

*To whom correspondence should be addressed; Magnetic Resonance Research Center, 300 Cedar St, PO Box 208043, New Haven, CT 06520-8043, USA; tel: 203-785-6148, fax: 203-737-1124, e-mail: dustin.scheinost@yale.edu

Schizophrenia is a severe global health problem, with over half of such patients experiencing auditory verbal hallucinations (AVHs). A better understanding of the neural correlates differentiating patients experiencing AVHs from patients not experiencing AVHs and healthy controls may identify targets that lead to better treatment strategies for AVHs. Employing 2 data-driven, voxel-based measure of functional connectivity, we studied 46 patients with schizophrenia or schizoaffective disorder (28 experiencing AVHs and 18 not experiencing AVHs). Twenty healthy controls matched for age, gender, ethnicity, education level, handedness, and estimated verbal intelligence were included for comparison. The intrinsic connectivity distribution (ICD) was used to model each voxel's connectivity to the rest of the brain using a Weibull distribution. To investigate lateralization of connectivity, we used cross-hemisphere ICD, a method that separates the contribution of each hemisphere to interrogate connectivity laterality. Patients with AVHs compared with patients without AVHs exhibited significantly decreased whole-brain connectivity in the medial prefrontal cortex and posterior cingulate cortex, less lateralized connectivity in left putamen, and more lateralized connectivity in left interior frontal gyrus. Correlations with Auditory Hallucination Rating Scale (AHRS) and post hoc seed connectivity analyses revealed significantly altered network connectivity. Using the results from all analyses comparing the patient groups and correlations with AHRS, we identified a potential AVH network, consisting of 25 nodes, showing substantial overlap with the default mode network and language processing networks. This network as a whole, instead of individual nodes, may represent actionable targets for interventions.

Key words: schizophrenia/default mode network/functional magnetic resonance imaging/language/computational psychiatry

Introduction

Schizophrenia is a severe global health problem,[1] with over half of patients experiencing auditory verbal hallucinations (AVHs).[2,3] Hallucinations remain a major treatment challenge and often produce high levels of distress, functional disability, and, in rare cases, violent acts including suicide.[4–9] A better understanding of the neural correlates differentiating patients experiencing AVHs from patients not experiencing AVHs and healthy controls (HCs) may lead to better treatment strategies for AVHs.

A growing consensus exists that disturbances in functional connectivity play an important role in the pathophysiology of schizophrenia.[10,11] Emerging studies have begun to investigate these disturbances in patients with AVHs.[12,13] Primarily using a priori defined regions of interest or "seeds," these studies have reported a complex range of altered connectivity for patients with AVHs compared with either patients without AVHs or HCs. Regions in auditory/language processing networks (including Heschl's gyrus, inferior frontal gyrus, Wernicke's area, and right hemisphere homologs) are common targets with elevated connectivity frequently reported.[14–18] Additionally, increased connectivity in the language processing network has been reported using components of interest generated from independent component analysis (ICA).[19] Finally, several studies have reported altered connectivity in regions of default mode network (DMN) including the temporoparietal junction

(TPJ) and posterior cingulate (PCC) using either seed-based[20,21] or ICA-based[19,22] methods. Nevertheless, the precise nature of these disturbances in schizophrenia and AVHs remains poorly understood.[23]

These earlier studies have examined connectivity in reference to specific seeds or components requiring a priori knowledge to select the regions or components of interest. An alternative strategy is to use data-driven, voxel-based methods that examine each voxel's connectivity to every other voxel in the brain. A potential advantage of such methods is that they are not constrained to a particular region or component and may lead to a more complete picture of the connectivity disturbances associated with AVHs. These methods have been successfully used to explore altered connectivity in a range of disorders including preterm birth,[24,25] AVHs in nonpsychotic individuals,[26] obsessive compulsive disorder,[27] and autism,[28] but not AVHs in individuals with schizophrenia.

The objective of this study is to more precisely characterize sites of altered functional connectivity associated with AVHs in patients with schizophrenia using data-driven, voxel-based methods. Whole-brain connectivity is investigated using the intrinsic connectivity distribution (ICD)[29] and cerebral lateralization of connectivity is characterized using cross-hemisphere ICD (chICD)[24] in patients with AVHs, patients without AVHs, and HCs. ICD summarizes a voxel's connectivity to the rest of the brain using a Weibull distribution, avoiding the need of arbitrary thresholds and assumptions of Gaussian distributions of previous methods.[25–28] ChICD is similar to ICD but separates the contribution of each hemisphere to interrogate connectivity laterality. Given the role of language in the generation of AVHs, the lateralization of language in the brain, and the reported altered connectivity between language homologs associated with AVHs,[15–18] we hypothesized that chICD would offer insights about AVHs complementary to ICD. Correlation between ICD and chICD and dimensions of hallucination experience were computed. Finally, seed connectivity maps were generated from regions of group differences to investigate which connections contributed to these observed differences. Together, these results provide evidence supporting a potential AVH network and that altered connectivity in schizophrenia is associated with AVHs.

Methods and Materials

All study procedures were approved by the Human Investigation Committee of the Yale University School of Medicine. All participants provided written, informed consent.

Participants

Patients met DSM-IV criteria for schizophrenia or schizoaffective disorder based on the Structured Clinical Interview for DSM-IV Axis I Disorders (SCID–I).[30] HCs without psychiatric history per assessment with the SCID–NP were enrolled. Participants were between 18 and 55 years old, and were excluded if they had a neurological disorder, current substance abuse, estimated intelligence quotient <80, or were left-handed. In total, 46 patients and 20 HCs were used for analysis. Patients with AVHs (AVHs+) were defined as patients experiencing AVHs at least once daily. Patients without AVHs (AVHs−) were defined as patients not experiencing AVHs within the prior 5 years. Patients experiencing AVHs in the past 5 years, but not daily were not enrolled. AVH status was determined through the SCID. All patients were taking antipsychotic medications. In order to assess effects of antipsychotic medication, chlorpromazine equivalent dosages were calculated for second- and first-generation antipsychotic drugs.[31–33]

Connectivity Preprocessing

Each participant underwent at least 6 runs within a single scanning session, each lasting 4 minutes, 6 seconds. Images were slice-time and motion corrected using SPM8 (http://www.fil.ion.ucl.ac.uk). Images were iteratively smoothed until the smoothness for any image had a full width half maximum of approximately 6 mm.[34] This iterative smoothing has been shown to minimize motion confounds associated with resting-state fMRI.[35] All further analysis was performed using BioImage Suite[36] unless otherwise specified. Several covariates of no interest were regressed from the data including linear and quadratic drift, a 24-parameter model of motion,[37] mean cerebral–spinal fluid signal, mean white matter signal, and mean global signal. The data were temporally smoothed with a zero mean unit variance Gaussian filter (cutoff frequency = 0.12 Hz). A gray matter mask was applied to the data. Each run was independently preprocessed and variance normalized. The 6 runs were then concatenated into 24.6 minutes of fMRI data. For subjects with more than 6 runs (4 subjects in total), the 6 runs with the lowest motion were included in analysis.

Intrinsic Connectivity Distribution Calculation

Functional connectivity of each voxel as measured by ICD was calculated for each individual participant as described previously.[29] This voxel-based functional connectivity measure involves correlating the time-course for any voxel with the time-course of every other voxel in the gray matter. Traditionally, these correlations are summarized using a network theory metric, such as degree or strength. Such metrics can be calculated from the distribution of correlations for any voxel x. First, $f(x, r)$ is defined as the distribution of the correlations (r) for the time-course at voxel x to the time-course at every other voxel in the brain and can be estimated by computing

the histogram of these correlations. Degree, based on a binary graph, can be estimated as the integral of this distribution from any threshold τ to 1, ie, $\int_{\tau}^{1} f(x,r)dr$. Strength can be estimated as the mean of this distribution or a distribution of transformed correlations, $\int_{-1}^{1} w(r)f(x,r)dr$, where $w(r)$ is the correlation coefficients or the Fisher transform of the correlation coefficients. In contrast, ICD models the entire corresponding survival function, $s(x,r)$, of $f(x,r)$, where $s(x,r)=\int_{r}^{1} f(x,u)du$. Each point on the survival function is simply degree, based on a binary graph, evaluated at that particular threshold, τ. The ICD approach parameterizes the change in a voxel's degree as the threshold defining whether voxels are connected (ie, correlation threshold) is increased. Previously,[29] we showed that it was sufficient to model this survival function as a stretched exponential decay with unknown variance parameter and shape parameter: $s(x,r,\alpha,\beta)=\exp(-(\frac{r}{\alpha})^{\beta})$, where x is the spatial location of a voxel, r is a correlation between 2 time-courses, α is the variance parameter, and β is the shape parameter. Modeling the survival function, $s(x,r)$, with a stretched exponential is equivalent to modeling the underlying distribution of correlation, $f(x,r)$, as a Weibull distribution. Thus, ICD models the distribution of correlations between a voxel and every other voxel in the brain, with α as the parameter of interest. No thresholds are needed to estimate the variance or model the distribution. This algorithm was performed for all voxels in the gray matter, resulting in a parametric image where the value of each voxel represents the alpha parameter obtained from model fitting.

Finally, each participant's map was normalized by subtracting the mean across all voxels and dividing by the standard deviation across all voxels. This normalization does not change the underlying connectivity pattern but ensures that all maps are equally scaled.[38]

Cross-hemisphere ICD

To explore lateralization of connectivity, we used a newly developed measure, chICD.[24] Like ICD, chICD involves correlating the time-course for a voxel x with every other time-course in the gray matter and then summarizing these correlations. However, chICD separates the contribution of each hemisphere to the ICD providing a measure of the laterality of a voxel's connectivity (Figure S1).

Specifically, the time-course for a voxel was correlated with the time-course for every other voxel in the hemisphere ipsilateral to that voxel. ICD was used to model the distribution of these correlations. This procedure was performed for every voxel, resulting in a map representing each voxel's connectivity to the same hemisphere, labeled ICD(*ipsi*). Similarly, a map representing a voxel's connectivity to the contralateral hemisphere was calculated, labeled ICD(*contra*). Both maps were normalized. Finally, to detect patterns of between hemisphere connectivity, the ICD(*ipsi*) and ICD(*contra*) maps were subtracted creating our chICD metric: chICD = ICD(*ipsi*) − ICD(*contra*).

For single group of chICD maps, a positive chICD value indicates that connectivity is relatively more lateralized to the ipsilateral hemisphere. A negative chICD value indicates that connectivity is relatively more lateralized to the contralateral hemisphere.

Common Space Registration

Single individual results were warped into MNI space using a series of linear and non-linear transformations. The functional data were linearly registered to the 2D anatomical images. The 2D anatomical image was linearly registered to the 3D MPRAGE image. The 3D MPRAGE images were non-linearly registered to an evolving group average template in an iterative fashion. This algorithm iterates between estimating a local transformation to align individual brains to a group average template and creating a new group average template based on the previous transformations.[39] All transformation pairs were calculated independently and combined into a single transform warping the single participant results into common space. This single transformation allows individual's results to be transformed to common space with only 1 transformation, reducing interpolation error.

Statistical Analysis

Connectivity maps were analyzed using voxel-wise, 2-sample t test for pairwise contrast. As the ICD (and chICD) parameters are found via regression analysis, we justify the use of parametric testing because the errors from the regression analysis are likely normally distributed and independent, given the reasonably large sample size used to estimate these parameters.[40] To control for task data, button press group (ie, button press or non-button press) was added as a covariate for all between group comparisons. Auditory Hallucination Rating Scale (AHRS)[41] was included as a regressor for a whole-brain analysis to examine the association between connectivity and hallucination severity. Anatomical locations were localized using the Yale Brodmann Area (BA) Atlas. Imaging results are shown at a cluster-level threshold of $P < .05$ family-wise error correction as determined by AFNI's 3dClustSim (version 16.3.05, which fixed the 3dClustSim "bug"). Monte Carlo simulations were performed using an estimate of smoothness from the data, cluster-generating threshold of $P < .01$, 10 000 iterations, and a gray matter mask.

Results

Participants

The 3 groups did not differ in terms of age, gender,

ethnicity, education, handedness, and estimated verbal intelligence (tables S1 and S2). Participants were scanned under resting-state conditions (n = 41) or during a sparse button press task (n = 25; see Supplemental Methods for full details). Participants scanned at rest were not asked about AVH experiences. All participants were part of a previous study[15] and 14 of the button press participants (n = 7 for AVH+, n = 7 for AVH−) were also part of another study.[42]

ICD and chICD Differences in AVHs+

Between group differences in ICD and chICD were examined to compare AVHs+, AVHs−, and HCs. Compared with AVHs−, AVHs+ showed significantly reduced connectivity in the medial prefrontal cortex (mPFC) and posterior cingulate cortex (PCC) (figure 1A). Compared with HCs, AVHs+ exhibited significantly greater connectivity in the parahippocampus and reduced connectivity in the thalamus (figure 1B).

For chICD, compared with AVHs−, AVHs+ showed significantly increased lateralization in left BA44 (inferior frontal gyrus or IFG) and in left BA19 and reduced lateralization of connectivity in the left putamen (figure 2A). Compared with HCs, AVHs+ exhibited significantly greater lateralization in the right thalamus and in the left motor cortex and reduced lateralization in the right motor cortex (figure 2B).

The ICD and chICD differences between AVHs+ and AVHs− remained significant when controlling for antipsychotic medication and diseases severity (figures S3 and S4). Additional control of button press data is presented in figure S6.

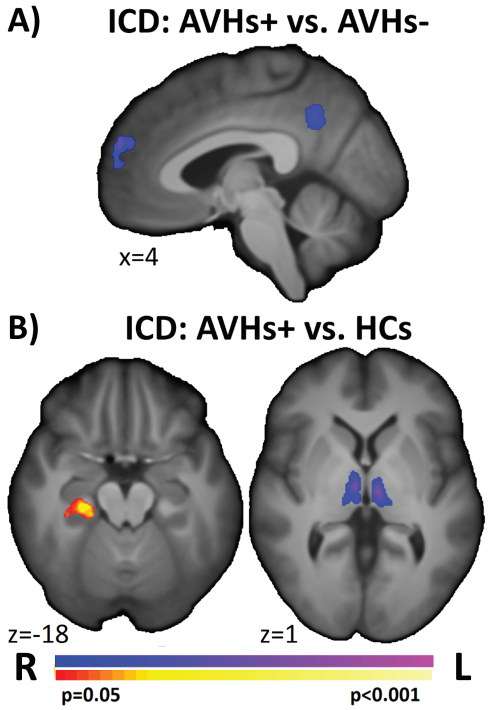

Fig. 1. ICD differences in patients with AVHs. Pairwise comparisons of AVHs+ to (**A**) AVHs− and (**B**) HCs suggest that the 2 patient groups differed in mPFC and PCC connectivity, and that AVHs+ differed from HCs in the thalamus and right parahippocampus. ICD, intrinsic connectivity distribution; AVH, auditory verbal hallucination; HC, healthy control; mPFC, medial prefrontal cortex; PCC, posterior cingulate cortex.

Correlation With AHRS

For AVHs+, significant correlations between AHRS and ICD were detected in the PCC, the right auditory cortex, and the right TPJ (BA40) as shown in figure 3A. Greater connectivity in the right auditory cortex and reduced connectivity in the PCC and in the right TPJ were associated with worse AVH symptoms. Additionally, a significant correlation (P < .05, corrected) between the AHRS and chICD was detected in left BA47 (IFG) such that reduced lateralization of connectivity was associated with worse AVH symptoms (figure 3B). AHRS was not correlated with antipsychotic medication, (r = 0.23; P = .24).

Post Hoc Seed Analysis Comparing AVHs+ and AVHs−

We performed post hoc seed connectivity analysis using mPFC, PCC, left BA44, left putamen, and left BA19 seeds derived from the AVHs+/AVHs− analysis (figures 1 and 2; see Supplemental Methods). For the mPFC, AVHs+ demonstrated significantly greater connectivity in the left putamen, the ACC/SMA, and left BA40 and reduced connectivity in the PCC and the mPFC/OFC (figure 4A). For the PCC, AVHs+ demonstrated significantly greater connectivity in the left IFG/insula, the ACC/SMA, and left BA40 and reduced connectivity in the PFC (figure 4B). For the left putamen, AVHs+ demonstrated significantly greater connectivity in mPFC, bilateral PFC, and in the left TPJ (BA21, BA39) and reduced connectivity in bilateral visual cortex and in right BA7 (figure 4C). For the left BA44, AVHs+ demonstrated significantly greater connectivity in mPFC, in bilateral PFC, in the left TPJ, and in the PCC and reduced connectivity in bilateral sensory-motor areas, in the right insula, in bilateral auditory cortex, and in bilateral fusiform (figure 4D). For left BA19, AVHs+ demonstrated significantly reduced connectivity in right temporal lobe and left parahippocampus (figure 4E). Exploratory comparisons of AVHs+/AVHs− and HCs are shown in figures S9 and S10.

Establishing a Potential AVH Network

To establish a potential AVH network, we computed the overlap of all significant AVHs+/AVH− group differences (ICD, chICD, and seed) and significant correlations with AHRS. While the seed results are not independent of the ICD/chICD results, they are important to consider in establishing a potential AVH network. These results provide the needed evidence that regions exhibiting ICD/

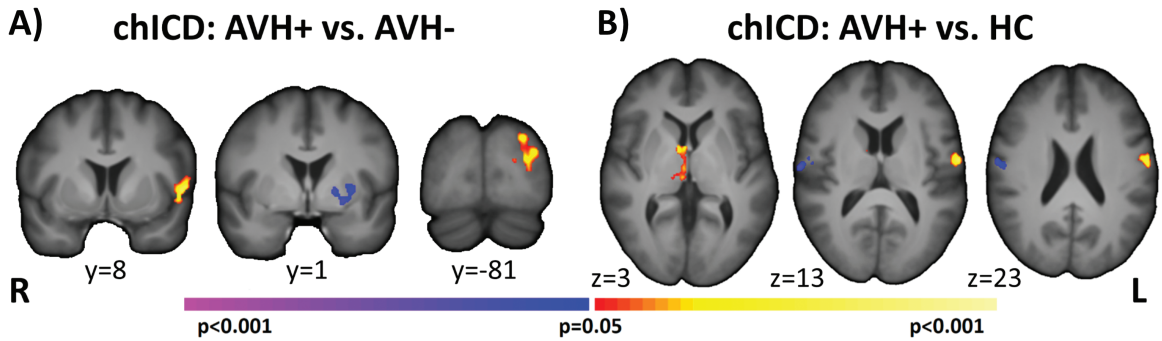

Fig. 2. chICD differences in patients with AVHs. Pairwise comparison of AVHs+ to (**A**) AVHs− and (**B**) HCs suggest that the 2 patient groups differed in left IFG, left putamen, and left BA19 connectivity and that AVHs+ differed from HCs in the thalamus and bilateral motor regions. All results shown at $P < .05$ corrected and in radiologic convention. chICD, cross-hemisphere intrinsic connectivity distribution; AVH, auditory verbal hallucination; HC, healthy control; IFG, inferior frontal gyrus.

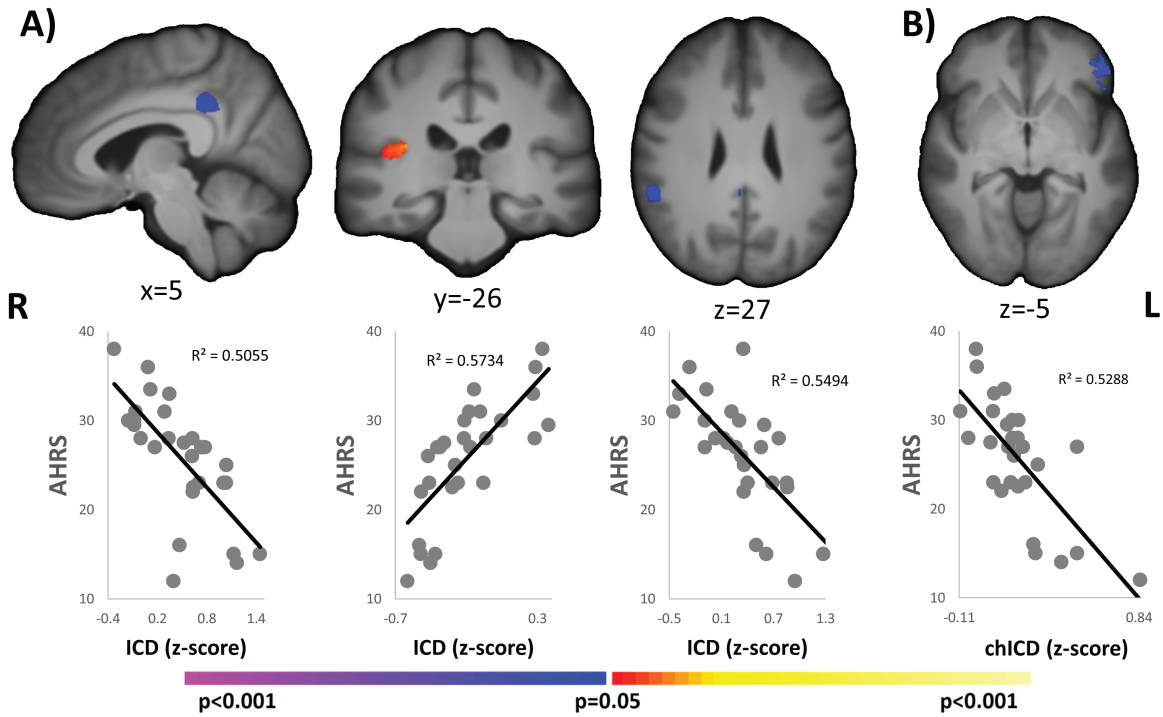

Fig. 3. Correlation with AHRS. **A.** For ICD, 3 regions (PCC, right auditory cortex, and right TPJ) were significantly ($P < .05$, corrected) correlated with AHRS. **B.** For chICD, left BA47 was significantly ($P < .05$ corrected) correlated with AHRS. Reduced connectivity or lateralization was associated with worse AVHs symptoms (higher AHRS) for the PCC, right TPJ, and left BA47. In contrast, increased connectivity in the right auditory cortex was associated with worse AVH symptoms (higher AHRS). All results shown at $P < .05$ corrected and in radiologic convention. AHRS, Auditory Hallucination Rating Scale; ICD, intrinsic connectivity distribution; PCC, posterior cingulate cortex; TPJ, temporoparietal junction; AVH, auditory verbal hallucination.

chICD differences do in fact interact with each other in a manner associated with AVH. As shown in figures 5 and S7, and table S3, these 25 nodes suggest a potential AVH network, with the greatest overlap in left hemisphere language regions and medial regions of the DMN. To further quantify which large-scale systems are involved in the potential AVH network, we used 8 large-scale brain networks as defined in Finn et al[43] (figure S8). As expected, greater than 36% of the AVH network was located in the anterior or posterior DMN. Additionally, 25% of the AVH network was located in the sensorimotor network, which includes auditory cortex and temporal lobe language regions. No other network made up greater than 15% of the AVH network (see table S4 for full details).

Discussion

Using recently developed voxel-wise connectivity methods, we identified patterns of cortical and subcortical connectivity that differed in patients with AVHs compared with patients without AVHs and HCs. Patients with AVHs compared with patients without AVHs exhibited decreased whole-brain connectivity in the mPFC and PCC, reduced

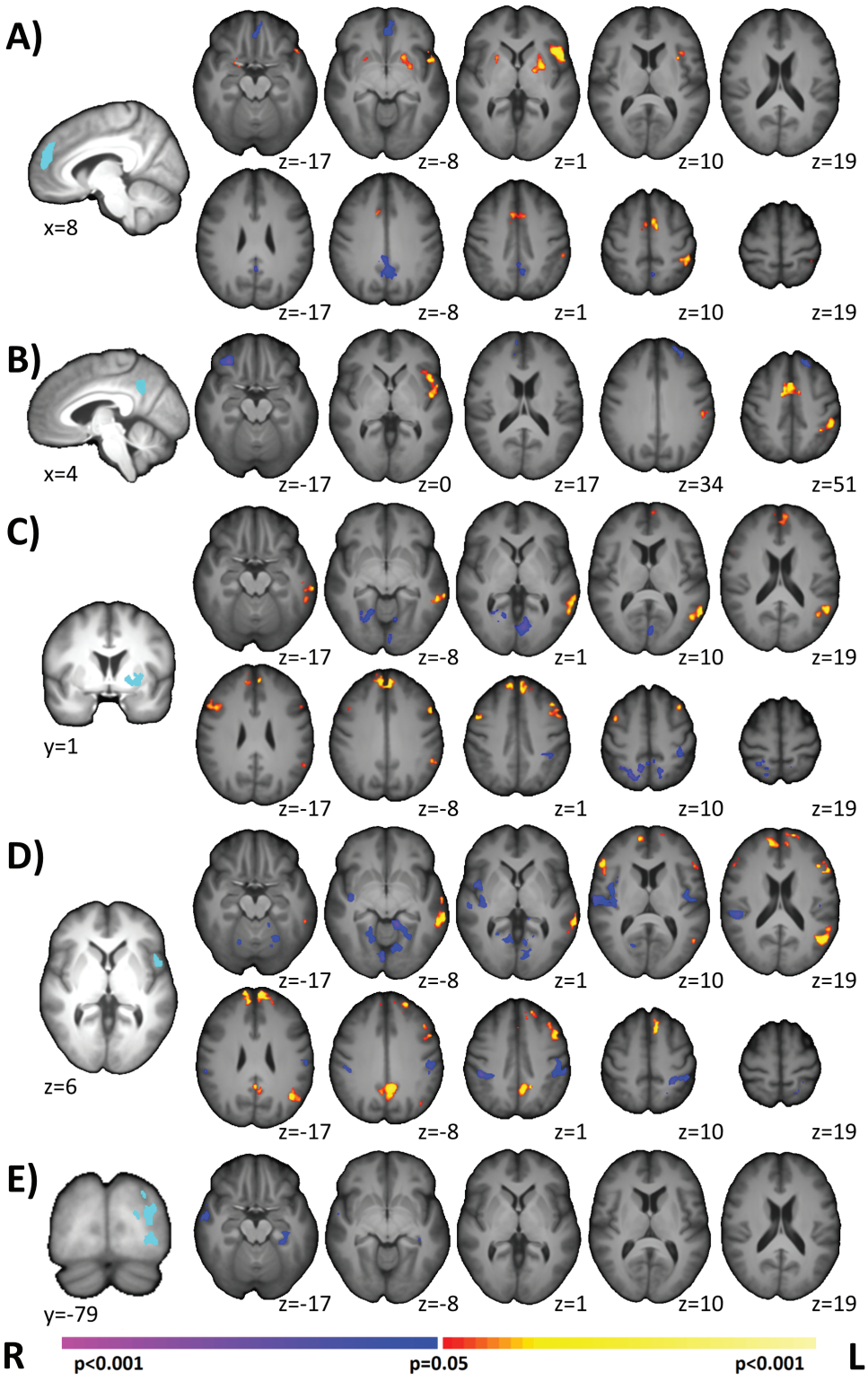

Fig. 4. Post hoc seed analysis comparing AVHs+ and AVHs−. Derived from our main group analysis, we performed post hoc seed connectivity analysis using the mPFC, the PCC, the left putamen, the left IFG, and left BA19 as seeds. **A.** Using the mPFC seed, AVHs+ demonstrated increased connectivity to the putamen and IFG, but decreased connectivity to the inferior mPFC. **B.** Using the PCC seed, AVHs+ demonstrated increased connectivity to the IFG, but decreased connectivity to PFC. **C.** Using the putamen seed, AVHs+ exhibited increased connectivity to the mPFC. **D.** Using the BA44 seed, AVHs+ exhibited increased connectivity to the mPFC. **E.** Using the BA19 seed, AVHs+ exhibited decreased connectivity to right temporal lobe and left parahippocampus. Together, these suggest that the interplays between these regions (mPFC, PCC, putamen, IFG) are important components for generating AVHs. Seed regions are shown in light blue on the left most column. All results shown at $P < .05$ corrected and in radiologic convention. AVH, auditory verbal hallucination; mPFC, medial prefrontal cortex; PCC, posterior cingulate cortex; IFG, inferior frontal gyrus; PFC, medial prefrontal cortex.

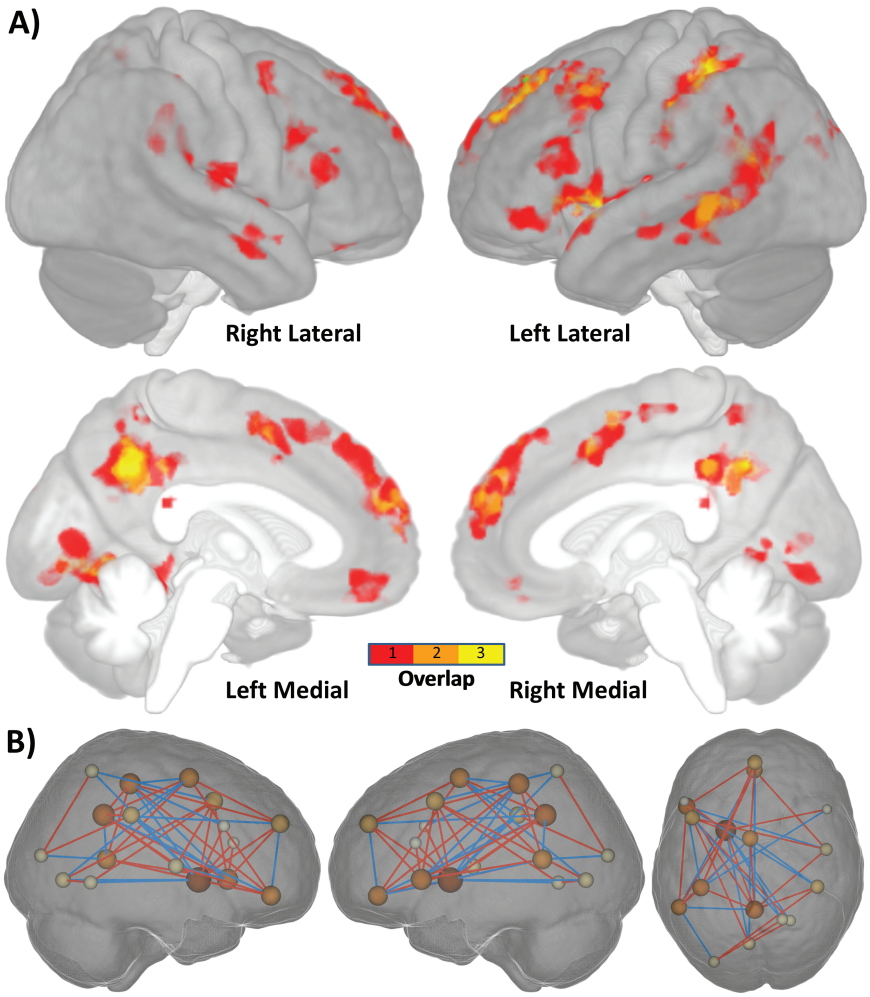

Fig. 5. Establishing a potential AVH network. **A.** To establish a potential AVH network, we computed the overlap of all significant AVHs+/AVH− group differences (ICD, chICD, and seed) and significant correlation with AHRS. This overlap suggests a potential AVH network, with main hubs (overlap ≥ 2) in left hemisphere language regions (Broca's and Wernicke's area) and medial regions of the DMN (mPFC and PCC). Not visualized in the surface render is the left putamen, another potential hub. **B.** Visualization of the connections in the AVHs network for that are different between AVHs+ and AVH− groups. Only connections with a difference greater than $r = 0.25$ are shown for visualization. Size of the spheres is proportional to the number of connections (or degree) for that node. Red lines indicate increased connectivity for AVHs+ and blue lines indicate decreased connectivity for AVHs−. AVH, auditory verbal hallucination; ICD, intrinsic connectivity distribution; chICD, cross-hemisphere ICD; AHRS, Auditory Hallucination Rating Scale; DMN, default mode network; mPFC, medial prefrontal cortex; PCC, posterior cingulate cortex.

lateralization in left putamen, and increased lateralization in left BA44 and left BA19. Correlations with AHRS and post hoc seed connectivity analysis emphasized altered connectivity in the DMN and language processing networks and suggested a potential AVH network.

The DMN, Putamen, and Language Processing Regions Form a Potential Hallucination Network

Our data-driven results highlight the mPFC, PCC, IFG, and putamen as key nodes that differed between patients with and without AVHs. Reduced whole-brain mPFC and PCC connectivity was associated with decreased connectivity within the DMN. This weakening of within-DMN connections is consistent with data from ICA and component-of-interest studies of connectivity in AVHs.[19,22,44] Increased BA44 lateralization was associated with increased connectivity to left hemisphere/midline regions and reduced connectivity to right hemisphere auditory cortex. Several studies have investigated IFG connectivity in patients with AVHs, producing a complex range of results, including increased and decreased connectivity.[16–18] This complexity is mirrored in our seed connectivity results, where several nodes and networks exhibited altered connectivity. The observed reduced lateralization of connectivity in the left putamen was likely associated not with a reduction in connectivity, but by an increase in connectivity to the contralateral medial and lateral PFC. A previous study has reported increased connectivity within the putamen between patients with AVHs compared with healthy controls using ICA,[45] consistent with our results. Additionally, putamen results are consistent

with our previous seed connectivity study using the current participants.[15] Overall, our data-driven regions represent plausible nodes in a potential AVH network.

Results obtained using these regions (mPFC, PCC, IFG, putamen) as seeds indicate the complex nature of the potential AVH network, as we observed consistent interactions between the different seeds. Our results indicate an increase in connectivity between language processing regions, the putamen, and the DMN with an accompanying decrease in connectivity between DMN nodes. These results are broadly consistent with the majority of functional connectivity studies and a recent meta-analysis of AVH[13,46] and suggest an AVH network. This network is similar to the "resting-state hypothesis" network,[47] where increased DMN activity influences auditory and language connectivity and leads to AVHs. However, our results suggest an overall reduced integrity or connectivity between nodes in the DMN consistent with other work.[19,22,44] Reduced connectivity within the DMN is not necessarily in conflict with previously reported increased activity in certain DMN nodes. Unconstrained increases in activity may be less synchronized across regions leading to a reduction of connectivity within the DMN. In addition, the complexity of the derived network (figure 4) may provide an explanation for the relative treatment-resistance of this symptom.[48] The numerous cortical and subcortical components may prevent network-wide functional shifts when only a few components are perturbed by standard treatments.

With the exception of the PCC, significant correlations between the AHRS and voxel-wise connectivity were observed in regions distinct from those detected in group comparisons. Nevertheless, these regions were located in the 2 main networks (language processing and DMN) consistent with the findings from group comparisons, underscoring the role of these nodes in forming a putative hallucination network. Decreased whole-brain connectivity in both the PCC and right TPJ was associated with increased AHRS (worse AVH symptoms), consistent with the weakening of the DMN presented here and elsewhere.[19,22,44] Similarly, decreased lateralization in left BA47 was associated with increased AHRS, which could be associated with either a decrease in connectivity to left hemisphere regions or an increase in connectivity to right hemisphere regions. Finally, increased global connectivity in right auditory cortex was associated with increased AHRS, consistent with models of AVHs.[47,49,50] Considering the observed distinction between regions associated with group differences and regions associated with symptoms reported here, the clinical relevance of these findings remains to be determined.

Methodological Considerations

We used 2, data-driven, voxel-wise methods to investigate AVHs in patients with schizophrenia. In contrast, the majority of studies on AVHs have focused on seed connectivity or ICA,[13] which requires a priori knowledge to select either regions or components of interest. The need for this a priori knowledge limits the ability of these approaches to identify altered connectivity beyond the prevailing hypothesis. As such, voxel-wise connectivity methods offer complementary information,[24,27–29] which can be used not only to confirm previous hypotheses, but also to generate new empirical data for theoretical methods.

These 2 methods measure different and unique aspects of brain organization. ICD reflects global, whole-brain connectivity, whereas chICD reveals hemispheric lateralization of connectivity. As shown here and elsewhere,[24,51,52] these 2 approaches offer complementary information regarding the functional organization of the brain and disruptions in this organization in clinical populations. While we used global signal regression in this study to help reduce motion and noise artifacts,[37,53] we have shown in several papers that ICD and chICD are not sensitive to GSR.[54,55]

Lastly, in contrast to the ~5 minutes of connectivity data traditionally acquired in other studies,[56,57] we acquired 24.6 minutes of data on all participants. There is a growing consensus that functional connectivity is highly dynamic,[58] and that a greater amount a data per subject is needed to fully capture this complexity.[43,59–61] The greater amount of data per subject in this study may lead to more robust and reliable group differences.[54]

Limitations

AVHs can be symptoms of disorders other than schizophrenia. However, we did not have a non-schizophrenia AVH group to determine if these connectivity differences are general to AVHs or specific to AVHs in schizophrenia. It is noteworthy that effects of antipsychotic medication were not found in our potential AVHs network using correlational methods (figure S2); however, medication effects may not scale linearly. Scan data for a portion of the subjects were not fully resting state, and, in some cases, included an occasional button press for the subject to indicate when they were experiencing a hallucination (for AVHs+) and random button presses (for AVHs− and HCs). The frequency of button presses across groups was not significantly different[42] and further analyses suggested that this did not drive our results (figures S5 and S6). Data from this study were from a previously published study,[15] which used a priori seeds in language regions (Broca's and Wernicke's areas). This study reported a corticostriatal loop consisting of the left IFG, bilateral Wernicke's areas, and bilateral putamen circuit underlying AVHs, similar to the chICD differences between AVHs+ and AVHs−. By using data-driven methods, we have extended this 5-node model to a 25-node model including several novel nodes in the DMN. While we performed several steps to minimize motion confounds, differences in motion between the patients and HCs approached significance. While resting-state fMRI is a powerful tool to map the functional organization of the brain, inherent limitations exist. If resting state is conceptualized

as a task state, different groups may have differences in "performing" rest.[62] For example, experiencing AVHs during rest may create a state difference between AVHs+ and AVHs−/HCs that is not accounted for in traditional resting-state analyses. As we did not sample participants' experience with post-scan interviews, we cannot control for such possible state differences. Lastly, it is unlikely that the identified regions represent the only nodes in an AVH network. Indeed, nodes hypothesized to be important for generating AVHs, such as limbic nodes,[63] were not highlighted by our methods.

Conclusions

We identified a network of altered cortical and subcortical connectivity associated with AVHs. Future work should continue to explore networks responsible for AVHs and develop interventions that target these networks as a whole, instead of individual nodes.

Supplementary Material

Supplementary material is available at *Schizophrenia Bulletin* online.

Funding

This work was supported by National Institute of Health (R01MH067073 and R01MH073673 to Dr Hoffman) and a National Alliance for Research on Schizophrenia and Depression Distinguished Investigator award to Dr Hoffman.

Conflict of interest: All authors declare no conflict of interest.

References

1. Knapp M, Mangalore R, Simon J. The global costs of schizophrenia. *Schizophr Bull*. 2004;30:279–293.
2. Andreasen NC, Flaum M. Schizophrenia: the characteristic symptoms. *Schizophr Bull*. 1991;17:27–49.
3. Mueser KT, Bellack AS, Brady EU. Hallucinations in schizophrenia. *Acta Psychiatr Scand*. 1990;82:26–29.
4. Ben-Zeev D, Morris S, Swendsen J, Granholm E. Predicting the occurrence, conviction, distress, and disruption of different delusional experiences in the daily life of people with schizophrenia. *Schizophr Bull*. 2012;38:826–837.
5. Hartley S, Barrowclough C, Haddock G. Anxiety and depression in psychosis: a systematic review of associations with positive psychotic symptoms. *Acta Psychiatr Scand*. 2013;128:327–346.
6. van Dongen JD, Buck NM, van Marle HJ. The role of ideational distress in the relation between persecutory ideations and reactive aggression. *Crim Behav Ment Health*. 2012;22:350–359.
7. Harkavy-Friedman JM, Kimhy D, Nelson EA, Venarde DF, Malaspina D, Mann JJ. Suicide attempts in schizophrenia: the role of command auditory hallucinations for suicide. *J Clin Psychiatry*. 2003;64:871–874.
8. Wong Z, Öngür D, Cohen B, Ravichandran C, Noam G, Murphy B. Command hallucinations and clinical characteristics of suicidality in patients with psychotic spectrum disorders. *Compr Psychiatry*. 2013;54:611–617.
9. Ten Velden Hegelstad W, Haahr U, Larsen TK, et al. Early detection, early symptom progression and symptomatic remission after ten years in a first episode of psychosis study. *Schizophr Res*. 2013;143:337–343.
10. Woodward ND, Cascio CJ. Resting-state functional connectivity in psychiatric disorders. *JAMA Psychiatry*. 2015;72:743–744.
11. Fornito A, Zalesky A, Pantelis C, Bullmore ET. Schizophrenia, neuroimaging and connectomics. *Neuroimage*. 2012;62:2296–2314.
12. Hoffman RE, Hampson M. Functional connectivity studies of patients with auditory verbal hallucinations. *Front Hum Neurosci*. 2011;6:6.
13. Alderson-Day B, McCarthy-Jones S, Fernyhough C. Hearing voices in the resting brain: a review of intrinsic functional connectivity research on auditory verbal hallucinations. *Neurosci Biobehav Rev*. 2015;55:78–87.
14. Shinn AK, Baker JT, Cohen BM, Ongür D. Functional connectivity of left Heschl's gyrus in vulnerability to auditory hallucinations in schizophrenia. *Schizophr Res*. 2013;143:260–268.
15. Hoffman RE, Fernandez T, Pittman B, Hampson M. Elevated functional connectivity along a corticostriatal loop and the mechanism of auditory/verbal hallucinations in patients with schizophrenia. *Biol Psychiatry*. 2011;69:407–414.
16. Sommer IE, Clos M, Meijering AL, Diederen KM, Eickhoff SB. Resting state functional connectivity in patients with chronic hallucinations. *PLoS One*. 2012;7:e43516.
17. Clos M, Diederen KM, Meijering AL, Sommer IE, Eickhoff SB. Aberrant connectivity of areas for decoding degraded speech in patients with auditory verbal hallucinations. *Brain Struct Funct*. 2014;219:581–594.
18. Diederen KM, Neggers SF, de Weijer AD, et al. Aberrant resting-state connectivity in non-psychotic individuals with auditory hallucinations. *Psychol Med*. 2013;43:1685–1696.
19. Wolf ND, Sambataro F, Vasic N, et al. Dysconnectivity of multiple resting-state networks in patients with schizophrenia who have persistent auditory verbal hallucinations. *J Psychiatry Neurosci*. 2011;36:366–374.
20. Vercammen A, Knegtering H, den Boer JA, Liemburg EJ, Aleman A. Auditory hallucinations in schizophrenia are associated with reduced functional connectivity of the temporo-parietal area. *Biol Psychiatry*. 2010;67:912–918.
21. Alonso-Solís A, Vives-Gilabert Y, Grasa E, et al. Resting-state functional connectivity alterations in the default network of schizophrenia patients with persistent auditory verbal hallucinations. *Schizophr Res*. 2015;161:261–268.
22. Jardri R, Thomas P, Delmaire C, Delion P, Pins D. The neurodynamic organization of modality-dependent hallucinations. *Cereb Cortex*. 2013;23:1108–1117.
23. Nature Editoral. A decade for psychiatric disorders. *Nature*. 2010;463:9.
24. Scheinost D, Lacadie C, Vohr BR, et al. Cerebral lateralization is protective in the very prematurely born. *Cereb Cortex*. 2015;25:1858–1866.
25. Constable RT, Vohr BR, Scheinost D, et al. A left cerebellar pathway mediates language in prematurely-born young adults. *Neuroimage*. 2013;64:371–378.

26. van Lutterveld R, Diederen KM, Otte WM, Sommer IE. Network analysis of auditory hallucinations in nonpsychotic individuals. *Hum Brain Mapp*. 2014;35:1436–1445.
27. Anticevic A, Hu S, Zhang S, et al. Global resting-state functional magnetic resonance imaging analysis identifies frontal cortex, striatal, and cerebellar dysconnectivity in obsessive-compulsive disorder. *Biol Psychiatry*. 2014;75:595–605.
28. Gotts SJ, Simmons WK, Milbury LA, Wallace GL, Cox RW, Martin A. Fractionation of social brain circuits in autism spectrum disorders. *Brain*. 2012;135:2711–2725.
29. Scheinost D, Benjamin J, Lacadie CM, et al. The intrinsic connectivity distribution: a novel contrast measure reflecting voxel level functional connectivity. *Neuroimage*. 2012;62:1510–1519.
30. First MB, Spitzer RL, Gibbon M, Williams Janet BW. *Structured Clinical Interview for DSM-5*. Arlington, VA: American Psychiatric Association; 2014.
31. Woods SW. Chlorpromazine equivalent doses for the newer atypical antipsychotics. *J Clin Psychiatry*. 2003;64:663–667.
32. Davis JM. Dose equivalence of the antipsychotic drugs. *J Psychiatr Res*. 1974;11:65–69.
33. Centorrino F, Eakin M, Bahk WM, et al. Inpatient antipsychotic drug use in 1998, 1993, and 1989. *Am J Psychiatry*. 2002;159:1932–1935.
34. Friedman L, Glover GH, Krenz D, Magnotta V; FIRST BIRN. Reducing inter-scanner variability of activation in a multicenter fMRI study: role of smoothness equalization. *Neuroimage*. 2006;32:1656–1668.
35. Scheinost D, Papademetris X, Constable RT. The impact of image smoothness on intrinsic functional connectivity and head motion confounds. *Neuroimage*. 2014;95:13–21.
36. Joshi A, Scheinost D, Okuda H, et al. Unified framework for development, deployment and robust testing of neuroimaging algorithms. *Neuroinformatics*. 2011;9:69–84.
37. Satterthwaite TD, Elliott MA, Gerraty RT, et al. An improved framework for confound regression and filtering for control of motion artifact in the preprocessing of resting-state functional connectivity data. *Neuroimage*. 2013;64:240–256.
38. Mitchell MR, Balodis IM, Devito EE, et al. A preliminary investigation of Stroop-related intrinsic connectivity in cocaine dependence: associations with treatment outcomes. *Am J Drug Alcohol Abuse*. 2013;39:392–402.
39. Scheinost D, Kwon SH, Lacadie C, et al. Alterations in anatomical covariance in the prematurely born. *Cereb Cortex*. 2017;27:534–543.
40. Scheinost D, Shen X, Finn E, Sinha R, Constable RT, Papademetris X. Coupled Intrinsic Connectivity Distribution analysis: a method for exploratory connectivity analysis of paired FMRI data. *PLoS One*. 2014;9:e93544.
41. Hoffman RE, Hawkins KA, Gueorguieva R, et al. Transcranial magnetic stimulation of left temporoparietal cortex and medication-resistant auditory hallucinations. *Arch Gen Psychiatry*. 2003;60:49–56.
42. Hoffman RE, Pittman B, Constable RT, Bhagwagar Z, Hampson M. Time course of regional brain activity accompanying auditory verbal hallucinations in schizophrenia. *Br J Psychiatry*. 2011;198:277–283.
43. Finn ES, Shen X, Scheinost D, et al. Functional connectome fingerprinting: identifying individuals using patterns of brain connectivity. *Nat Neurosci*. 2015;18:1664–1671.
44. Rotarska-Jagiela A, van de Ven V, Oertel-Knöchel V, Uhlhaas PJ, Vogeley K, Linden DE. Resting-state functional network correlates of psychotic symptoms in schizophrenia. *Schizophr Res*. 2010;117:21–30.
45. Sorg C, Manoliu A, Neufang S, et al. Increased intrinsic brain activity in the striatum reflects symptom dimensions in schizophrenia. *Schizophr Bull*. 2013;39:387–395.
46. Jardri R, Pouchet A, Pins D, Thomas P. Cortical activations during auditory verbal hallucinations in schizophrenia: a coordinate-based meta-analysis. *Am J Psychiatry*. 2011;168:73–81.
47. Northoff G, Qin P. How can the brain's resting state activity generate hallucinations? A 'resting state hypothesis' of auditory verbal hallucinations. *Schizophr Res*. 2011;127:202–214.
48. Shergill SS, Murray RM, McGuire PK. Auditory hallucinations: a review of psychological treatments. *Schizophr Res*. 1998;32:137–150.
49. Cho R, Wu W. Mechanisms of auditory verbal hallucination in schizophrenia. *Front Psychiatry*. 2013;4:155.
50. Northoff G. Are auditory hallucinations related to the brain's resting state activity? A 'Neurophenomenal Resting State Hypothesis'. *Clin Psychopharmacol Neurosci*. 2014;12:189–195.
51. Buckner RL, Sepulcre J, Talukdar T, et al. Cortical hubs revealed by intrinsic functional connectivity: mapping, assessment of stability, and relation to Alzheimer's disease. *J Neurosci*. 2009;29:1860–1873.
52. Cole MW, Pathak S, Schneider W. Identifying the brain's most globally connected regions. *Neuroimage*. 2010;49:3132–3148.
53. Power JD, Plitt M, Laumann TO, Martin A. Sources and implications of whole-brain fMRI signals in humans. *Neuroimage*. 2017;146:609–625.
54. Scheinost D, Finn ES, Tokoglu F, et al. Sex differences in normal age trajectories of functional brain networks. *Hum Brain Mapp*. 2015;36:1524–1535.
55. Qiu M, Scheinost D, Ramani R, Constable RT. Multi-modal analysis of functional connectivity and cerebral blood flow reveals shared and unique effects of propofol in large-scale brain networks. *Neuroimage*. 2017;148:130–140.
56. Woodward ND, Karbasforoushan H, Heckers S. Thalamocortical dysconnectivity in schizophrenia. *Am J Psychiatry*. 2012;169:1092–1099.
57. Anticevic A, Haut K, Murray JD, et al. Association of thalamic dysconnectivity and conversion to psychosis in youth and young adults at elevated clinical risk. *JAMA Psychiatry*. 2015;72:882–891.
58. Hutchison RM, Womelsdorf T, Allen EA, et al. Dynamic functional connectivity: promise, issues, and interpretations. *Neuroimage*. 2013;80:360–378.
59. Anderson JS, Ferguson MA, Lopez-Larson M, Yurgelun-Todd D. Reproducibility of single-subject functional connectivity measurements. *AJNR Am J Neuroradiol*. 2011;32:548–555.
60. Laumann TO, Gordon EM, Adeyemo B, et al. Functional system and areal organization of a highly sampled individual human brain. *Neuron*. 2015;87:657–670.
61. Birn RM, Molloy EK, Patriat R, et al. The effect of scan length on the reliability of resting-state fMRI connectivity estimates. *Neuroimage*. 2013;83:550–558.
62. Buckner RL, Krienen FM, Yeo BT. Opportunities and limitations of intrinsic functional connectivity MRI. *Nat Neurosci*. 2013;16:832–837.
63. Amad A, Cachia A, Gorwood P, et al. The multimodal connectivity of the hippocampal complex in auditory and visual hallucinations. *Mol Psychiatry*. 2014;19:184–191.